Frequency Response Function (FRF) Technique for the Diagnosis of Suspension System

Moamar Hamed[1*], Mohammed Elrawemi[1] , Feng Gu[2]

[1] moamar.ehmeid@gamil.com, [2] mselrawemi@elmergib.edu.ly, [3] f.gui@hud.ac.uk

[1] Department of Mechanical Eng; , College of Engineering, Elmergib University, Libya
[3] Centre for Efficiency and Performance Engineering, University of Huddersfield, UK

*Corresponding author email: moamar.ehmeid@gamil.com

ABSTRACT

Some of the common faults associated with suspension components are damaged or leaking shock absorbers, spring weakness, wearing down of the pivot and bushing. To investigate these problems, a seven degree-of-freedom (7-DOF) model has been developed, for a full vehicle, using MATLAB. In the simulation, the suspension faults have been considered via the damage caused to the shock absorbers (dampers) and the faults were seeded by reducing the damper coefficient by 25%, 50% and 80%.

Frequency Response Function (FRF) technique was used to develop conditioned monitoring tools for suspension faults and detects the level of damping coefficients. To validate the model and evaluate the FRF technique stated in this study, experimental investigation was carried out on 4-post-test rig at the University of Huddersfield in order to measure the FRFs of the suspension for different damping setting.

The results demonstrate that, the shape of the frequency response depends on the damping coefficient (c), since low damping coefficients lead to good isolation properties of the vehicle mass in the mid- to high frequency range, but also leads to high amplitudes of the acceleration in the range of the natural frequency of the vehicle body (sprung mass). Therefore, FRFs analyses provide an effective monitoring of the suspension and to detect the level of change in damping coefficients.

Keywords: suspension system, Frequency response Function (FRF), damping coefficients, Suspension Faults

1 Introduction

During the last ten years, a variety of FFT-based two channel digital spectrum analysers have become commercially available which can make frequency response measurements[1]. The Frequency Response Function is a fundamental measurement that isolates the inherent dynamic properties of a mechanical structure [2]. The FRF describes the input-output relationship between two points on a structure as a function of frequency. An FRF is a measure of how much acceleration response a structure has at an output Degree Of Freedom (DOF), per unit of excitation force at an input DOF. The (FRF) is, in general, a complex valued function or waveform defined over a frequency range and includes both a real and imaginary component that can be resolved into magnitude and phase. Therefore, the process of identifying parameters from this type of measurement is commonly called curve fitting, or parameter estimation. Several experimental modal parameters such as natural frequencies, mode shapes and associated damping ratios can be extracted from a set of FRF measurements. Frequency Response Function Model can be Considered as a linear system as represented by the diagram in Figure 1 .

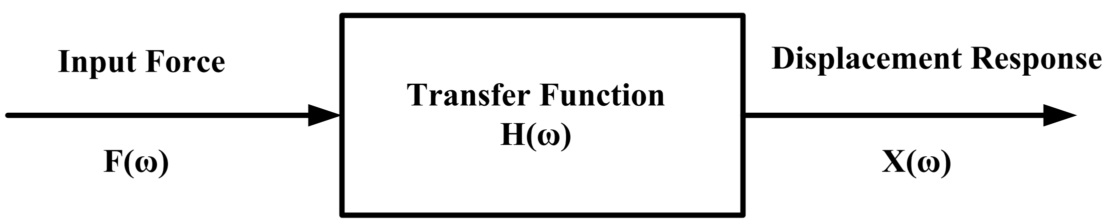

Figure 1: *Frequency Response Function Model [3]*

Where: F (ω) is the input force as a function of the angular frequency ω . H (ω) is the transfer function. X (ω) is the displacement response function. Each function is a complex function, which may also be represented in terms of magnitude and phase. Each function is thus a spectral function. There are numerous types of spectral functions. For simplicity, consider each to be a Fourier transform [3].

The relationship in Figure 1 can be represented by the following equations

$$\mathrm{X}(\omega) = H(\omega) \cdot F(\omega) \qquad (1)$$

$$\mathrm{H}(\omega) = \frac{\mathrm{X}(\omega)}{\mathrm{F}(\omega)} \qquad (2)$$

Similar transfer functions can be developed for the velocity and acceleration responses.

2 Frequency Response Function for single degree of freedom (SDOF) system

For simplicity a single-degree-of-freedom system subjected to a force excitation has been considered [3] as shown in Figure 2 .

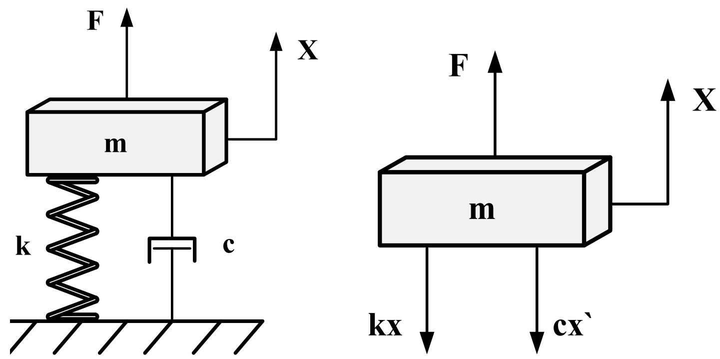

Figure 2: *Single-degree-of-freedom system and free-body diagram [3]*

Where m = mass, c = viscous damping coefficient, k = stiffness, x = absolute displacement of the mass, F = applied force.

Summation of forces in the vertical direction

$$\Sigma F = m\ddot{x} \tag{1}$$

$$m\ddot{x} + c\dot{x} + kx = F \tag{2}$$

$$\ddot{x} + (c/m)\dot{x} + (k/m)x = F/m \tag{3}$$

By convention,

$$(c/m) = 2\xi f_n \tag{4}$$

$$(k/m) = f_n^2 \tag{5}$$

Where f_n is the natural frequency in (radians/sec) and ξ is the damping ratio

Substituting the convention terms into equation (5)

$$\ddot{x} + 2\xi f_n \dot{x} + f_n^2 x = f_n^2 F/k \tag{6}$$

The Fourier transform of each side of equation (9) may be taken to derive the steady-state transfer function for the absolute response displacement, as shown in Reference 1. After many steps, the resulting transfer function is

$$\frac{X(\omega)}{F(\omega)} = \left[\frac{1}{k}\right]\left[\frac{f_n^2}{f_n^2 - f^2 + j(2\xi f f_n)}\right] \tag{7}$$

This transfer function, which represents displacement over force, is sometimes called the reacceptance function [4]. The transfer function can be represented in terms of magnitude and phase angle ϕ as following:

$$\frac{X(\omega)}{F(\omega)} = \left[\frac{1}{k}\right]\left[\frac{f_n^2}{\sqrt{\left(f_n^2 - f^2\right)^2 + \left(2\xi f f_n\right)^2}}\right] \tag{8}$$

$$\frac{X(\omega)}{F(\omega)} = \left[\frac{1/m}{\sqrt{\left(f_n^2 - f^2\right)^2 + \left(2\xi f f_n\right)^2}}\right] \tag{9}$$

$$\phi = \arctan\left[\frac{2\xi f f_n}{f_n^2 - f^2}\right] \tag{10}$$

The mobility function (Velocity / Force) can be considered as

$$\frac{V(\omega)}{F(\omega)} = \left[\frac{1}{k}\right]\left[\frac{j f f_n^2}{f_n^2 - f^2 + j(2\xi f f_n)}\right] \tag{11}$$

$$\left|\frac{V(\omega)}{F(\omega)}\right| = \left[\frac{1}{k}\right]\left[\frac{f\, f_n^2}{\sqrt{\left(f_n^2 - f^2\right)^2 + \left(2\xi\, f\, f_n\right)^2}}\right] \tag{12}$$

$$\left|\frac{V(\omega)}{F(\omega)}\right| = \left[\frac{1}{m}\right]\left[\frac{f}{\sqrt{\left(f_n^2 - f^2\right)^2 + \left(2\xi\, f\, f_n\right)^2}}\right] \tag{13}$$

$$\theta = \arctan\left[\frac{-f_n^2 + f^2}{2\xi f_n}\right] \tag{14}$$

The acceleration function (Acceleration / Force) can be presented as

$$\frac{A(\omega)}{F(\omega)} = \left[\frac{1}{k}\right]\left[\frac{-f^2\, f_n^2}{f_n^2 - f^2 + j\left(2\xi\, f\, f_n\right)}\right] \tag{15}$$

$$\left|\frac{A(\omega)}{F(\omega)}\right| = \left[\frac{1}{k}\right]\left[\frac{-f^2\, f_n^2}{\sqrt{\left(f_n^2 - f^2\right)^2 + \left(2\xi\, f\, f_n\right)^2}}\right] \tag{16}$$

$$\left|\frac{A(\omega)}{F(\omega)}\right| = \left[\frac{1}{m}\right]\left[\frac{-f^2}{\sqrt{\left(f_n^2 - f^2\right)^2 + \left(2\xi\, f\, f_n\right)^2}}\right] \tag{17}$$

$$\alpha = -\pi + \arctan\left[\frac{2\xi f_n}{f_n^2 - f^2}\right] \tag{18}$$

The basic assumption for single-mode approximations is that in the vicinity of a resonance, the response is due primarily to that single mode. The resonant frequency can be estimated from the frequency response data (illustrated in Figure 3) by observing the frequency at which any of the following trends occur:

- The magnitude of the frequency response is a maximum.
- The response lags the input by 90° phase.

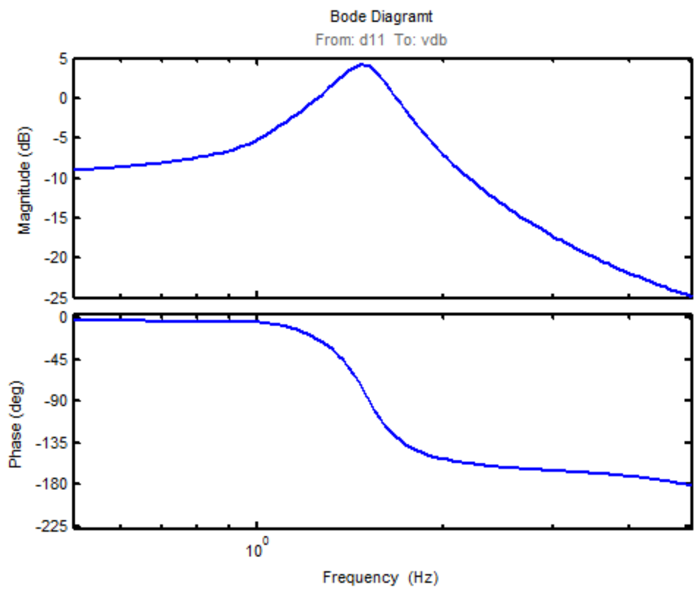

Figure 3: *Bode Diagram magnitude and phase versus frequency for SDOF system*

It can be noted that the height of the resonant peak is a function of damping. Damping serves to minimize or reduce the amplitude at the natural frequency and is often regarded as a measure of the frictional energy that is defined by the molecular characteristics of the structure. The level of damping on a system also has an effect on the magnitude of the amplitude at the resonant frequency of a system [5]. This is shown in figure 4. It was discussed earlier that the height of the resonant peak is a function of damping. The damping factor can be estimated by the half power method or other related mathematical or graphical method. In the half-power method, the damping is estimated by determining the sharpness of the resonant peak. It can be shown from Figure 4 that damping can be related to the width of the peak between the half-power points: points below and above the resonant peak at which the response magnitude is .7071 times the resonant magnitude.

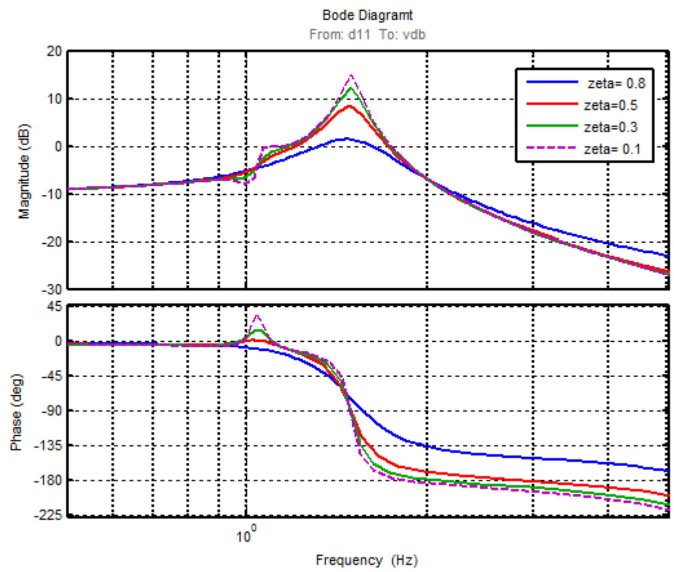

Figure 4: *Bode diagram for different damping ratio (zeta)*

3 Experimental investigation for FRF measurements

Early detections of abnormal events in automotive suspension systems can reduce the damage caused to the vehicle in driving situations, in addition to improving passenger comfort and security. The performance of a vehicle is often downgraded due to the appearance of faults with the suspension. The common faults associated with suspension components are damaged or leaking shock absorbers, spring weakness, and damage to the main support member assembly. These faults can cause reduced operating efficiency and cause potential damage to the vehicle.

In order to evaluate suspension condition monitoring (CM) techniques stated in this study and also to measure the FRFs of the suspension for different damping setting, experimental work was carried out on 4-post-test rig at the University of Huddersfield. During the tests, the car is induced with the fault of damaged shock absorber, by replacing the front passive shock absorbers with adjustable shocks from SPAX Company; these shock absorbers can offer different damping force, and also more safer to perform the tests. The test was conducted to measure the vibration response of the car body and the vibration of the platform (shaker), the vibration signals were collected for baseline conditions and for different damping coefficients of suspension. For this purpose, the two front shock absorbers of the car were replaced with two adjustable shock absorbers from SPAX Company; these shock absorbers can offer different damping force.

This test consists of three main parts a commercial car, a measurement system (vibration sensors, amplifiers, data acquisition and portable laptop) and the 4-post simulator system (shaker). Figure 5 is an illustrative photograph of the 4-post-test rig and the tested car used in this study. This section comprises the experimental facilities and test procedures.

In practice, the models produced by modal testing often have poor quality due to factors inherent in the measurement. One of the sources of a lack of precision in modal testing is the errors caused by mechanical devices such as accelerometers, suspension springs and stingers.

Figure 5: *the tested car (Vauxhall Zafira)*

4 Experimental Facilities

4.1 The tested car specification

In this study a Vauxhall ZAFIRA car, 4 cylinder engines, with a front wheel drive and tyre model LT245/75R16E has been used, the specifications of the tested car are shown in the table 1. To evaluate the condition monitoring techniques stated in this study and also to measure the FRFs of the suspension for different damping setting, the two front shock absorbers of the car were replaced with adjustable shock absorbers (struts from SPAX Company), these shock absorbers can offer different damping forces and all adjustments can made without any dismantling of components, making it simpler, faster and easier to obtain ultimate set-up for the suspension. The SPAX shock absorbers have 28 stages of damping force adjustment. This allows a wide range of adjustment to suit different driving style and road conditions. Struts shock absorbers (adjuster at the top) are adjustable in the rebound.

To obtain the perfect set up for the car and passengers, the manufacturer recommended initially setting all the shock absorber to fully soft (anti-clockwise), and then by adjusting up in 4 click increments, the conditions of the shock absorber will be changed from soft to hard. Figure 6shows the SPAX shock absorber.

Table 1: *specification of the tested car*

Body style	MPV 5-Doors	Height	1634 mm
Driven Wheels	Front (FWD)	Wheel Base	2694 mm
Length	4317 mm	Weight	1448 kg
Width	1742 mm		

Figure 6: *Adjustable shock absorber from SPAX*

4.2 Measurement instrumentation

4.2.1 Accelerometers

Accelerometers are inertial measurement devices that convert mechanical motion into a voltage signal. The signal is proportional to the vibration's acceleration using the piezoelectric principle. The piezo-electric accelerometer is the most commonly used transducer for vibration measurement.

This sensor consists of a piezoelectric crystal and small mass normally enclosed in a protective metal case. When the accelerometer is subjected to vibration, the mass exerts a varying force on the piezoelectric crystal, which is directly proportional to the vibratory acceleration. The charge produced by the piezoelectric crystal is proportional to the varying vibratory force. The charge output is measured in Pico-coulombs per g (pC/g) where g is the gravitational acceleration. Some sensors have an internal charge amplifier, while others have an external charge amplifier. The charge amplifier converts the charge output of the crystal to a proportional voltage output in mV/g.

In this research, a piezoelectric accelerometer (model CA-YD-104T) is used to measure the vibration of the test car. These accelerometers are used on most vibrating surfaces because their mass does not significantly affect the movement of the surface, and possess a wide enough frequency range appropriate for measuring automobile vibration (0.5Hz to over 7 kHz). They are environmentally robust enough to withstand the conditions existing on cars and are of an adequate sensitivity. However, they do have an upper temperature limit of about 120C^{o}due to their inbuilt microelectronics. The accelerometers are connected to an external charge amplifier YE5857A-1 providing power to the accelerometers and amplifying the charge signals. The amplified output signals of this device are sent to the data acquisition system for recording and analysis. Figure 7 shows photos of both the accelerometer and the preamplifier. A detailed specification of the accelerometer used in this work is summarized in table 2.

Figure 7: *accelerometer and amplifier*

Table 2: *specification of the accelerometer*

Vibration sensors	Sensor 1	Sensor 2
Model	CA-YD-104T	CA-YD-104T
Serial number	07143	07213
Sensitivity	3.243 pc/ms^{-2}	3.573 pc/ms^{-2}
Frequency range	0.5 to 7000 Hz	0.5 to 7000 Hz
Temperature	-20 to 120 ºC	-20 to 120 ºC

4.2.2 Data acquisition system

The Model YE7600 has 4 channels each channel has its own measurement converter A/D (analog/digital), which can be set to the sampling frequency in the range 96 kHz. Converters working in parallel are synchronized by the measure, giving the possibility of the simultaneous acquisition on these 4 channels. This type of data acquisition is adequate for monitoring vibration signal as its high sampling frequency which is sufficient for keeping the key information of original analog signal during the analog-to-digital conversion. This data acquisition is easily connected to the portable laptop by USB wire for recording and analysing the data.

Figure 8 *Data acquisition equipment (model YE6261B)*

4.3 Test procedures

Testing was carried out on the tested car. The vibration signals were collected using two accelerometers (CA-YD-104T) mounted on the car body and the base of the platform (shaker), as illustrated in Figure 5. The two identical accelerometers were used to measure FRFs. One of the main considerations regarding the accelerometers is that of the accessibility of installing them. To measure the vertical acceleration of the car body, the sensors mounted on the car include: (1) a vibration sensor mounted on the upper mounting point of the front left shock absorber where the mounting surface is flat and where the sensor can be mounted easily by gluing. This is common for many condition monitoring applications which place sensors in close proximity to vibration sources in order to acquire good vibration response characteristics. Then the same sensor 1 was moved and mounted in the same position on the upper mounting point of the front right shock absorber, figure 9 (a) shows the position of the front sensors. For measuring the vibration in the rear car body, the same sensor 1 also moved and fixed on the end of each rear corner of the car body, where the sensor can be close to the rear shock absorbers, figure 9 (b) illustrated the position of the rear sensors . Sensor 2 is represented to measure the acceleration in vertical direction, generated by the platform .The accelerometer catching on the platform was made in rigid assembly by sticking with Superglue as shown in the Figure 9 (c).

Figure 9 (a) *Sensor position on front wheels (b) sensor position on rear wheels and (c) sensor position on the shaker base.*

The most fundamental aim of the test was to obtain the acceleration (vibration) response of the suspension system to calculate the FRFs of the vehicle. For this purpose, multiple measurements were made when the oscillatory motion was generated by oscillating each platform separately. Determination of dynamic response has been made for the front left, the front right, the rear left and the rear right wheel respectively. The vehicle is exposed to a linear (sine sweep) frequency with the amplitude of 5 mm and a frequency range of 0.5 to 8Hz was sufficient to include the vehicle body characteristics, the frequency was increased by the rate of 0.03Hz/sec. The signals were collected and measured simultaneously and the sampling rate of data acquisition was 3000Hz. For each measurement, 765000 data points were collected and recorded in 255 seconds.

Two different experimental have been conducted, Test 1 was to measure the FRFs of the vehicle under normal operating conditions, meaning the suspension was running without any induced faults and the tyre pressure of each wheel was applied to a normal pressure of 2.2bar before starting the tests. Each test was repeated three times for each corner to ensure that the data consists of the interested characteristics of the tested vehicle.

Test 3 was performed to measure the FRFs of the vehicle for different damping coefficients, the aim of this test is to evaluate the on-road tests, for this purpose the front shock absorbers of the vehicle were replaced with adjustable shock absorbers (struts from SPAX Company). This test was conducted in two different cases, in the test (2) the damping setting of the front left shock absorber was changed in four cases as presented in Table 3. In the test (3), the damping setting of the front right shock absorber was changed in four cases as shown in the table 4. Each test has repeated three times and after each test, the data acquired were viewed and imported to MATLAB files for further processing.

Table 3: *Experimental set up*

Test (2.1)	Damping conditions		Test (2.2)	Damping conditions	
	Front left	Front right		Front left	Front right
A	Fully soft	Fully soft	A	Fully soft	Fully soft
B	2-pteps hard	Fully soft	B	Fully soft	2-pteps hard
C	4-pteps hard	Fully soft	C	Fully soft	4-pteps hard
D	Fully hard	Fully soft	D	Fully soft	Fully hard

Fully soft that mean the shock absorber is in the baseline conditions, 2-steps hard, 4-steps hard and fully hard refer to decreases in the damping coefficients as a result of the faults in the damping system, which may induced to the system as a result of one or more of the following factors: worn seals, a reduction in the oil volume due to leakages, broken mounts and extruded or worn bushings section should extend, not repeat, the background to the article already dealt with in the Introduction and lay the foundation for further work.

5 Results and Discussion

It is well known in general that each machine will produce its own spectrum of frequencies. If the baseline vibration of a healthy machine is compared to the signal of a similar machine running under similar conditions, any increase over the baseline at any forcing frequency can indicate the presence of abnormalities in the machine. The baseline vibration signals (waveform) were recorded by the accelerometers of 765000 data points for 225 seconds. Baseline raw data of the acceleration response and FRF corresponding to the vehicle body as output sensor 1 and the front left platform as input sensor 2 are shown in Figures10. It can be noted that, in swept frequency signal, the frequency is proportional to variations of time.

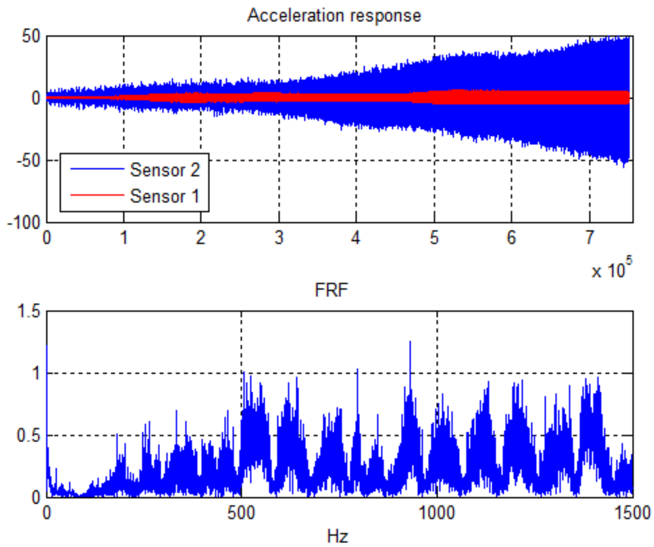

Figure 10: *Acceleration response and FRF corresponding to the vehicle body sensor 1 and the platform sensor 2*

To evaluate the proposed conditioned monitoring method for suspension faults, which has been developed in this research, to evaluate the on-road tests and to detect the level of damping coefficients, the Frequency Response Function (FRF) technique was used. The FRF is a fundamental measurement that isolates the inherent dynamic properties of a mechanical structure and also describes the input-output relationship between two points on a structure as a function of frequency.

Figure 11 shows the amplitude-frequency characteristic curves for the baseline conditions of the suspension in the four corners of the vehicle front left (FL), front right (FR), rear left (RL) and rear right (RR), the road tests have shown some differences in the energy transmitted to the car body at each corner. In this figure, the four corners of the vehicle can show a notable difference in the vibration signals. It can be noted that, the damping was higher in the front left corner than the front right corner, and the rear corners also produce some differences. This can be identifying the reason behind the differences in the energy transmitted to the vehicle in the on-road tests, which cause of some disagreements between the simulation and the experimental results.

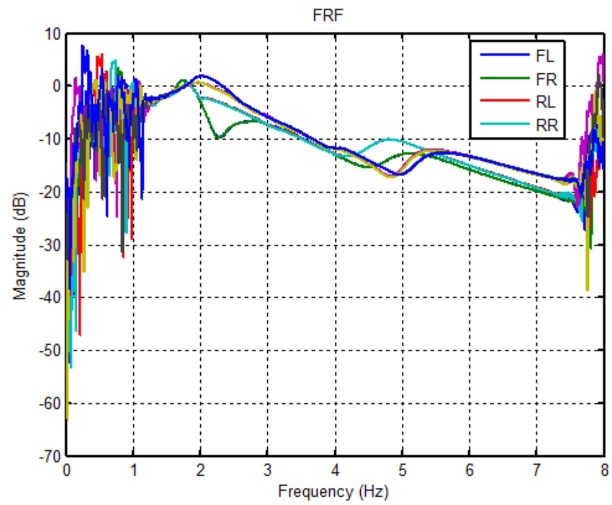

Figure 11: *FRFs for the four corner of the vehicle*

Figure 12 shows the acceleration ratio of the vehicle body (sprung mass) to the platform input with 4 damping conditions (fully soft, 2-steps hard, 4-steps hard and fully hard) as presented in the table 4. Theoretically, when the level of this ratio is around unity (0 dB) with no phase difference, the force between the wheel and the platform is said to be the static load and the tyre deflection is constant.

The plots reveal that increasing the damping coefficient reduces the value of the response magnitude for excitation frequencies of the vehicle body natural frequency. From this, it can be concluded that in the frequency range close to the natural frequency of the vehicle body, a high damping is required. However, lower damping is required to provide better vibration isolation in the mid- to high frequency range.

The same can be said for the figure 11, which presents the FRFs of the vehicle body and the platform for the front right corner of the vehicle. However, the differences in this side are slightly less than the differences in the left side.

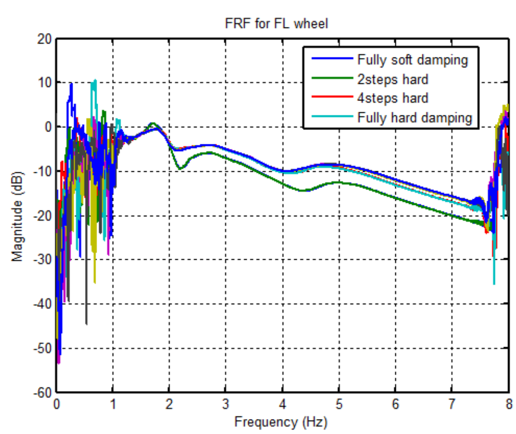

Figure 12: *FRFs for the front left wheel with different damping coefficients*

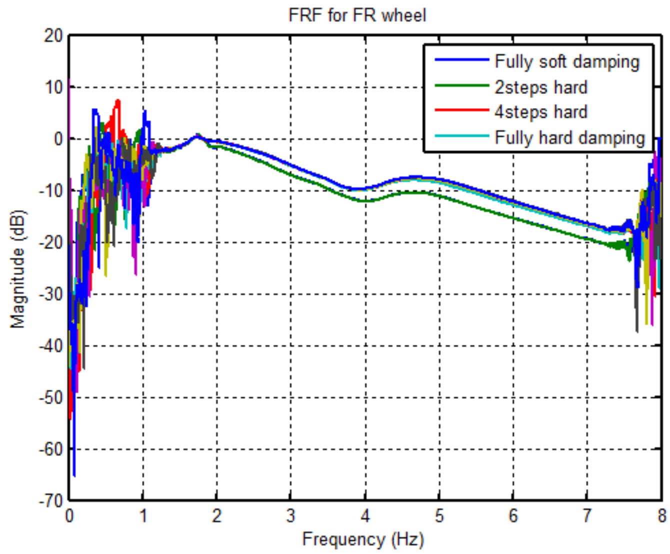

Figure 13: *FRFs for the front right wheel with different damping coefficients*

6 Conclusion

System being similar to those for the linear viscous damping, the isolation ability between the bounce mode and the wheel-hop mode is worse for the non-linear damping. This means the cubic damping might cause the sprung mass to have high level of response for the intermediate excitation frequencies.

One can say that with the higher force compressing the tyre, more grips will be obtained. The tyre is vibrating when either the ratio is not equal to unity or unity but with phase difference. If the tyre stiffness is too soft this will cause much vibration in the deflection of the tyre due to the undulating surface input. This can lead the wheel to vibrate against the stiffness of the tyre. This might result in poor quality of road holding, since to obtain good road holding the tyre deflection.

References

[1] M. H. Richardson and D. L. Formenti, “Parameter estimation from frequency response measurements using rational fraction polynomials,” in Proceedings of the International Modal Analysis Conference, 1982, pp. 167–182.

[2] H. Herlufsen, “Modal Analysis using Multi-reference and Multiple-Input Multiple-Output Techniques,” Brüel Kjær Appl. Note, 2004.

[3] T. Irvine, “an Introduction to Frequency Response Functions,” Rapp. Coll. Eng. Comput. Sci., 2000.

[4] H. Packard, “The fundamentals of modal testing,” application note 243-3, 1997.

[5] S. Cornelius and G. B. Paresh, “Practical Machinery Vibration Analysis and Predictive Maintenance,” 2004.